Solubilization of rare earth oxides in the eutectic LiCl–KCl mixture at 450 °C and in the equimolar CaCl2–NaCl melt at 550 °C

ARTICLE *in* JOURNAL OF ELECTROANALYTICAL CHEMISTRY · MARCH 2003

Impact Factor: 2.87 · DOI: 10.1016/S0022-0728(03)00092-5

5 AUTHORS, INCLUDING:

Yolanda Castrillejo
Universidad de Valladolid
82 PUBLICATIONS **1,183** CITATIONS
SEE PROFILE

E. Barrado
Universidad de Valladolid
159 PUBLICATIONS **3,061** CITATIONS
SEE PROFILE

Available online at www.sciencedirect.com
SCIENCE DIRECT®
Journal of Electroanalytical Chemistry 545 (2003) 141–157
Journal of Electroanalytical Chemistry
www.elsevier.com/locate/jelechem

Solubilization of rare earth oxides in the eutectic LiCl–KCl mixture at 450 °C and in the equimolar $CaCl_2$–NaCl melt at 550 °C

Y. Castrillejo [a,*], M.R. Bermejo [a], E. Barrado [a], A.M. Martínez [a,1], P. Díaz Arocas [b]

[a] Dpto de Química Analítica, Facultad de Ciencias, Universidad de Valladolid, Prado de la Magdalena s/n, 47005 Valladolid, Spain
[b] CIEMAT, Dept. de Fisión Nuclear, Avda. Complutense 22, Madrid 28040, Spain

Received 1 August 2002; received in revised form 22 January 2003; accepted 30 January 2003

Abstract

Solubilization studies of rare earth oxides and oxohalides have been carried out in the eutectic LiCl–KCl melt at 450 °C and the equimolar $CaCl_2$–NaCl mixture at 550 °C. First, chlorinating conditions were predicted by comparing the E–pO^{2-} diagram of the different rare earth-O compounds to that of several chlorinating gaseous mixtures. Then, experimental solubilization tests were performed by using pure HCl and Cl_2 gases and the chlorinating $Cl_2(g)+C(s)$ mixture. In order to build up the potential–acidity diagrams, stability of the oxidation states of rare earths (RE being La, Ce, Nd, Pr and Y), standard potentials of the different redox couples as well as solubility products of oxides and oxychlorides were determined in both molten chlorides at the temperatures studied. Oxidation states (III) and (0) were found to be stable in both molten chlorides for all REs and (II) in the case of neodymium. The standard potential values of the different redox couples were also determined by combining both potentiometry and cyclic voltammetry and then allowed us to obtain the activity coefficients of $RECl_3$ compounds in the molten media. It was found that RE(III) cations were less solvated by the chloride ions in the calcium melt, which could be explained by formation of $CaCl_4^{2-}$ ions. Moreover it was demonstrated that at a given working temperature, the rare earth cations with higher polarizability (higher charge to ionic radius values) are also more solvated by the melt. Solubilization tests of RE–O samples showed that in the case using gaseous Cl_2 as chlorinating agent, the kinetics of the chlorinating reaction were much slower than those for gaseous HCl.

Keywords: Molten chlorides; Lanthanides; Rare earths; Yttria-stabilized zirconia electrode; E–pO^{2-} diagrams; Solubilization test

1. Introduction

Molten salts, and particularly molten chlorides, are well known as good reaction media for performing selective solubilization or precipitation in chemical reactions, and have already been proposed as a promising route for the treatment of raw materials and subsequent recovery of valuable metals by electrowinning [1].

Pyrochemical separation processes in molten media have more recently been proposed as a promising option in the nuclear fuel cycle for the future [2–6], mainly due to progress in the assessment of new concepts for transmutation and the corresponding fuel cycles [7], and several processes have already been developed for the recovery of minor actinides from spent metallic, nitride and oxide nuclear fuels and high level radioactive liquid wastes [8,9].

The work presented here is part of a broader project focused on the separation of actinides from lanthanides—the more difficult fission products to separate due to their similar chemical properties—from oxide nuclear fuels, which involves the dissolution of some of the products in a molten chloride using chlorinating agents.

Some authors have used the so-called generalized Pourbaix type diagrams E–pO^{2-} (or potential–acidity diagrams) for metal–O compounds to predict separating conditions of the different metals from the sample [10–

* Corresponding author.
E-mail address: ycastril@qa.uva.es (Y. Castrillejo).
[1] Present address: Department of Materials Technology, Sem Sælands vei 6, 7491 Trondheim, Norway.

0022-0728/03/$ - see front matter
doi:10.1016/S0022-0728(03)00092-5

21].The construction of these diagrams can be made by combining thermodynamic and experimental data.

In this work, chlorinating conditions of rare earths (RE being La, Ce, Nd, Pr and Y)–O compounds were extracted by comparing the corresponding diagrams to that from some chlorinating mixtures based on gaseous Cl_2 and HCl. The eutectic LiCl–KCl mixture at 450 °C and the equimolar $CaCl_2$–NaCl at 550 °C were used as reaction media. In some cases the working temperatures were increased in order to check the influence of temperature on the kinetics of the chlorinating reactions.

2. Experimental

The appropriate amounts of the chloride mixtures (equimolar $CaCl_2$–NaCl and eutectic LiCl–KCl, analytical grade) were melted in a 100 cm^3 Pyrex or alumina crucible placed in a quartz cell inside a Taner furnace. A West 3300 programmable device controlled the temperature of the furnace to ± 2 °C. The working temperature was measured with a thermocouple protected by an alumina tube inserted into the melt. All handling of the salts was carried out in a glove box under an argon atmosphere.

The purification of the mixtures was performed according to the method proposed by Laitinen et al [22] and was described previously [16,23].

The pO^{2-} indicator electrode consisted of a tube of yttria-stabilized zirconia, supplied by Degussa France or Interbil Spain, filled with molten $CaCl_2$–NaCl or LiCl–KCl solution containing oxide and silver ions (3×10^{-2} and 0.75 mol kg^{-1} respectively) into which a silver wire was immersed (inner reference Ag | AgCl).

The reference electrode consisted of a silver wire (1 mm diameter) dipped into a silver chloride solution (0.75 mol kg^{-1}) in the $CaCl_2$–NaCl or LiCl–KCl molten mixture, contained in a Pyrex tube. Potentials were measured by reference to the Ag | AgCl couple.

Two different types of RE–working electrodes were used: wires or foils of the pure RE ($\geqslant 99.9\%$) and tungsten wires covered by the RE generated 'in situ' by coulometry at constant potential.

In the electrochemical experiments, working and counter electrodes of 1 mm diameter tungsten wires were used, and performed by a PAR 273A potentiostat/galvanostat. The emf was measured by means of a high resistance multimeter (Fluka 45).

Solutions of the RE(III) were obtained by adding the corresponding amounts of solid $RECl_3$, which was stored in the glove box until its use without further purification.

3. Results and discussion

3.1. Determination of the oxoacidity constant of the HCl/H_2O system

As it has been shown previously [10,24–27], the equilibrium constant, $K_{H_2O/HCl}$, of the reaction:

$$H_2O(g) + 2Cl^- \Leftrightarrow O^{2-} + 2HCl(g) \quad (1)$$

$$K_{H_2O/HCl} = \frac{P_{HCl}^2[O^{2-}]}{P_{H_2O}[Cl^-]^2} \quad (2)$$

in a molten medium M, allows us to characterize the oxoacidity properties of M.

Processes, like solubilization of oxides by chlorination in molten salts, can be predicted a priori by determining the oxoacidity properties of the molten mixtures.

The equilibrium constant $K_{H_2O/HCl}$ can be determined experimentally by imposing certain partial pressures of HCl and H_2O over the molten media. This can be easily done by bubbling argon gas through thermostated HCl solutions [27]. The partial pressures of HCl and H_2O are fixed by the temperature and concentration of the HCl solutions [28], which can be accurately determined by acid–base titration with a Na_2CO_3 solution.

The potential values between the zirconia and the reference electrode correspond to the cell

$$\underset{\text{indicator electrode}}{Ag|AgCl(ds)\ \text{molten salt}\ Na_2CO_3(ds)|ZrO_2 - Y_2O_3} \underset{\text{reference electrode}}{|\text{molten salt}_{pO2^- \text{measured}}|\text{pyrex}|AgCl(ds)|Ag} \quad (3)$$

and follows the Nernstian expression:

$$E = A + \frac{2.3RT}{2F} pO^{2-} \quad (4)$$

According to Eq. (2), pO^{2-} is given by:

$$pO^{2-} = pK_{(H_2O/HCl)} + \log \frac{P_{HCl}^2}{P_{H_2O}} \quad (5)$$

Fig. 1a and Fig. 2a show the variations of E versus $[\log(P_{HCl}^2/P_{H_2O})]$ obtained in both melts.

In order to correlate E with pO^{2-} values, calibration of the zirconia electrode was performed by addition of known amounts of solid Na_2CO_3 or BaO (Fig. 1b, Fig. 2b), a method that has been already proved to work [13,23,29–31]. Then $K_{H_2O/HCl}$ can be determined from the plot pO^{2-} versus $[\log(P_{HCl}^2/P_{H_2O})]$, according to Eq. (5) (Fig. 3). The values so obtained in both melts and in different experiments are given in Table 1. In the case of the eutectic LiCl–KCl mixture at 450 °C, the $K_{H_2O/HCl}$ value is in very good agreement with that obtained by Picard et al. [29] and Lisy and Combes [32] who obtained 10.30 and 10.33 respectively.

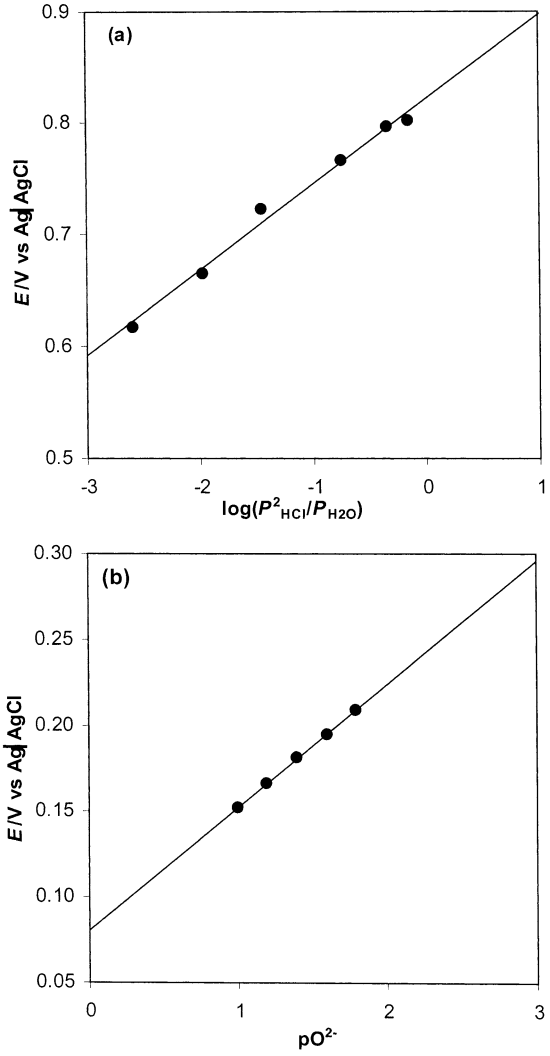

Fig. 1. Emf values between the zirconia and reference electrode obtained by potentiometry at zero current in the eutectic LiCl–KCl melt at 450 °C. (a) When imposing different partial pressures of HCl and H_2O in the molten chloride; (b) when adding known amounts of solid Na_2CO_3.

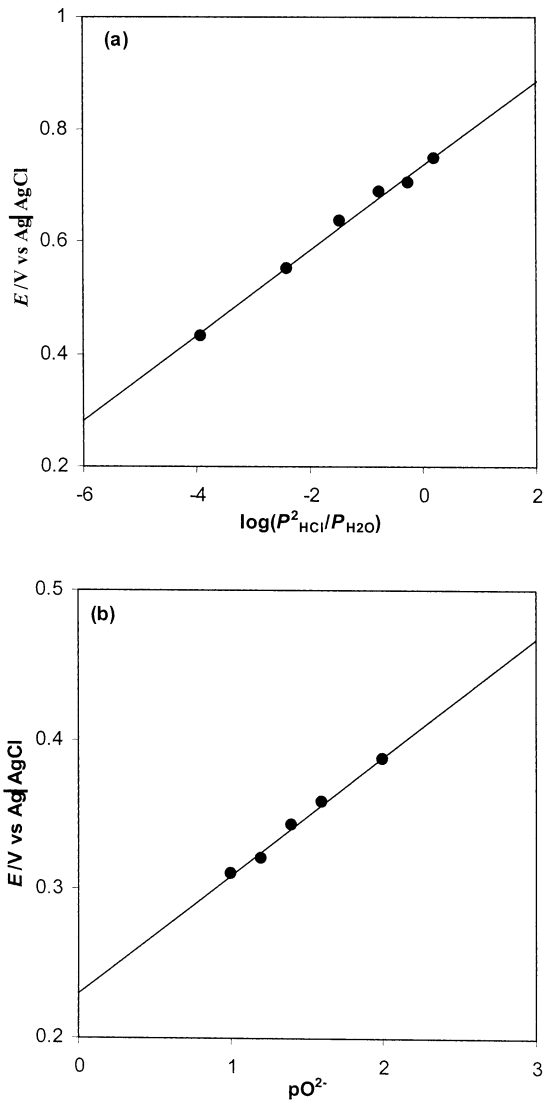

Fig. 2. Emf values between the zirconia and reference electrode obtained by potentiometry at zero current in the equimolar $CaCl_2$–NaCl melt at 550 °C. (a) When imposing different partial pressures of HCl and H_2O in the molten chloride; (b) when adding known amounts of solid Na_2CO_3.

Figs. 4a and b show the good response of the electrode in the range of pO^{2-} studied, and the wide working range of the zirconia electrode in both molten media.

Table 1
Values of $K_{H_2O/HCl}$ obtained in both molten media

Eutectic mixture LiCl–KCl at 450 °C			Equimolar $CaCl_2$–NaCl melt at 550 °C		
Experiment #	$pK_{H_2O/HCl}$	Error range	Experiment #	$pK_{H_2O/HCl}$	Error range
1	10.70	10.36–11.05	1	6.20	6.10–6.23
2	9.70	9.22–10.04	2	6.34	6.04–6.65
3	10.35	10.09–10.55	3	6.34	6.13–6.55
			4	6.12	5.91–6.33
Average	10.25	10.25±0.53		6.25	6.25±0.17

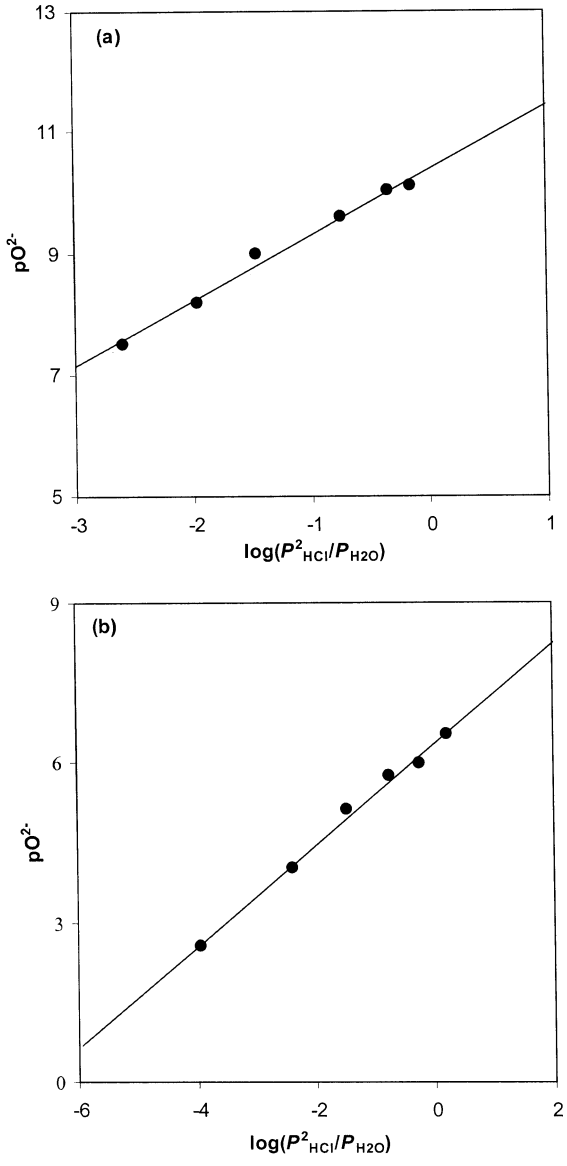

Fig. 3. Variation of pO^{2-} with $[\log(P^2_{HCl}/P_{H_2O})]$. (a) In the eutectic LiCl–KCl melt at 450 °C; (b) in the equimolar $CaCl_2$–NaCl melt at 550 °C.

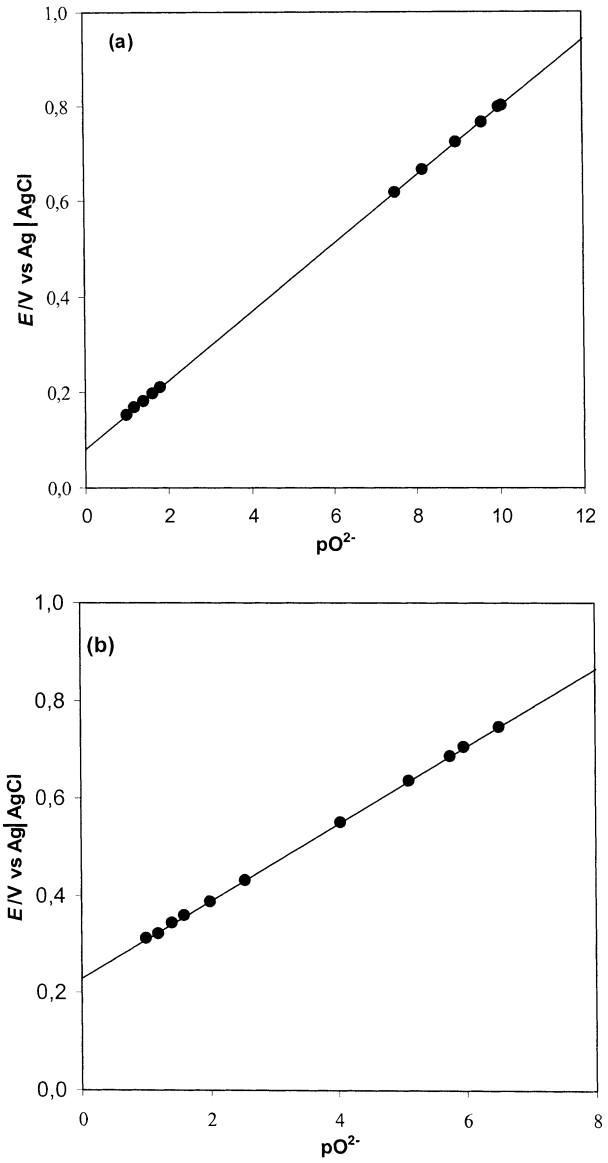

Fig. 4. Variation of the YSZE potential in a wide pO^{2-} range. (a) In the eutectic LiCl–KCl melt at 450 °C; (b) in the equimolar $CaCl_2$–NaCl melt at 550 °C.

3.2. Solubilization studies of RE–O compounds

3.2.1. Stable oxidation states of the rare earth elements in the molten chlorides studied

The stable oxidation states of the rare earth elements studied (La, Ce, Nd, Pr and Y) were identified by different electrochemical techniques.

In all cases, typical cyclic voltammograms obtained on a tungsten working electrode in the molten solutions containing RE(III) ions (Fig. 5) (RE = Ce, La, Pr, Y) showed a single group of signals, A/A′, in the potential range close to the lower limit of the melt (electrodeposition of liquid lithium or sodium). The shape of the A/A′ system is characteristic of the formation of a new phase, which can be associated with the RE metal.

However, in the case of Nd two groups of signals were obtained when sweeping a Nd(III) solution in the molten chlorides negatively (Fig. 6a and b). B/B′ corresponding to the soluble–soluble Nd(III)/Nd(II) exchange and A/A′ corresponding to the Nd(II)/Nd(0) system. One can see that Nd(II) ions are more stable in the equimolar $CaCl_2$–NaCl melt than in the eutectic LiCl–KCl.

The upper limit of the melt corresponds to chlorine evolution (Cl_2/Cl^- system) in both molten chlorides. The absence of any other electrochemical wave indicated that Ce(IV)/Ce(III) and Pr(IV)/Pr(III) potentials are beyond the range accessible, proving the oxidating power of Ce(IV) and Pr(IV) ions in both melts.

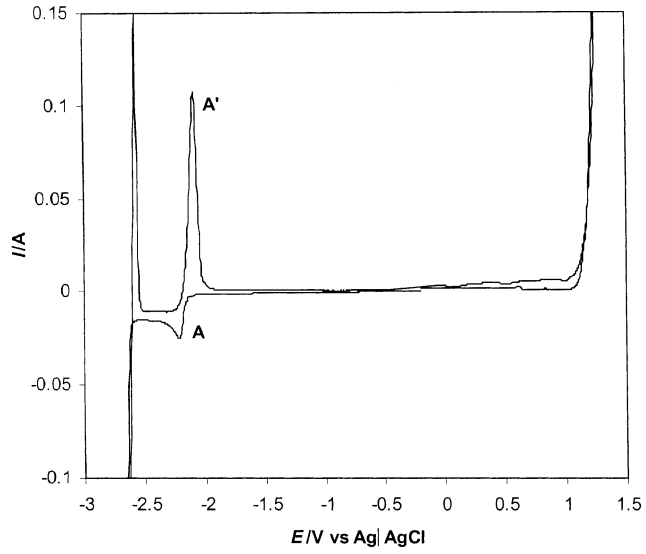

Fig. 5. Example of a typical cyclic voltammogram obtained in the eutectic LiCl–KCl mixture at 450 °C containing a RE(III) solution (in this case 7.5801×10^{-5} mol cm^{-3} $PrCl_3$). Tungsten working electrode ($S = 0.22$ cm^2).

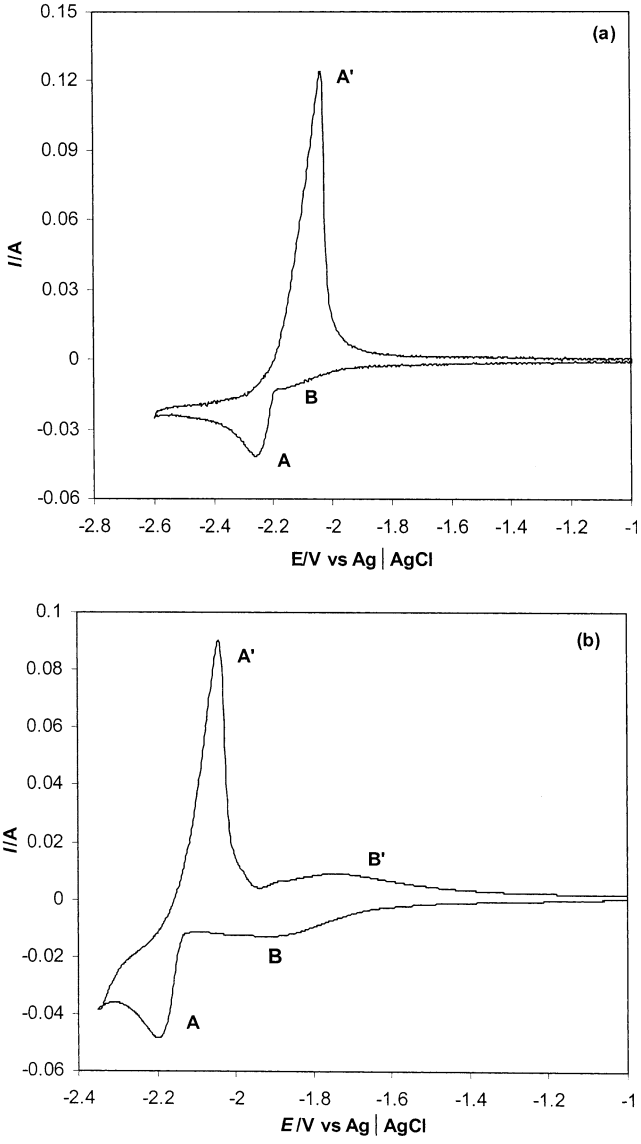

Fig. 6. Cyclic oltammogram obtained with a NdIII solution in: a eutectic LiClKCl melt at 450C 1.2140104 molcm3 NdCl3; b equimolar CaCl2NaCl melt at 550C 1.9835104 molcm3 NdCl3.

It is known that rare earth metals are soluble in their molten chlorides [33–36] which is responsible for the low current efficiency in the electrolysis, moreover mixtures of rare earth chlorides and rare earth metals give rise to electronic conduction, which may influence electrochemical measurements. The work of Keneshea and Cubicciotti [35] indicates that the solubility of lanthanum in its liquid trichloride is 9% at 826 °C and 11% at 914 °C. Therefore, dilute solutions of $RECl_3$ in the LiCl–KCl or $CaCl_2$–NaCl melts are expected to show very low metal solubility.

The above results were confirmed by square wave voltammetry and chronopotentiometry (Fig. 7), being identical in both the eutectic LiCl–KCl melt and the equimolar $CaCl_2$–NaCl mixture, showing that the only stable oxidation states of the studied rare earths are (III) and (0) and (III), (II) and (0) in the case of neodymium.

3.2.2. Experimental determination of the standard potentials in solution of the RE(III)/RE(0)couple. Activity coefficients of RE(III). Study of the influence of the temperature

The standard potential $E^{\circ}_{1\ \mathrm{RE(III)/RE(0)}}$ in solution can be determined by measuring the equilibrium potential of a RE electrode in the molten chloride containing different concentrations of RE(III) ions with respect to the Ag | AgCl reference electrode. The expression of the galvanic cell is:

$$\mathrm{Ag(s)}\left|\begin{matrix}\mathrm{AgCl(ds)},\\ \text{molten salt}\end{matrix}\right|\left|\begin{matrix}\text{molten salt},\\ \mathrm{RECl_3(ds)}\end{matrix}\right|\left|\mathrm{RE(s)}\right. \qquad (6)$$

The emf is given by:

$$\begin{aligned}\mathrm{emf} &= E_{\mathrm{RE}} - E_{\mathrm{ref}} \\ &= E^{\circ}_{1\ \mathrm{RE(III)/RE(0)}} + 2.3\frac{RT}{3F}\log[\mathrm{RE(III)}] - E_{\mathrm{ref}} \end{aligned} \qquad (7)$$

The variation of the cell emf versus the logarithm of the RE(III) concentration when using both a tungsten wire covered by RE or a foil/wire of pure RE, was a straight line whose slope is very close to the theoretical one predicted by the Nernst equation (0.0477 in LiCl–KCl at 450 °C and 0.0544 in $CaCl_2$–NaCl at 550 °C). The values of the standard potentials were determined by the intercept of the plots.

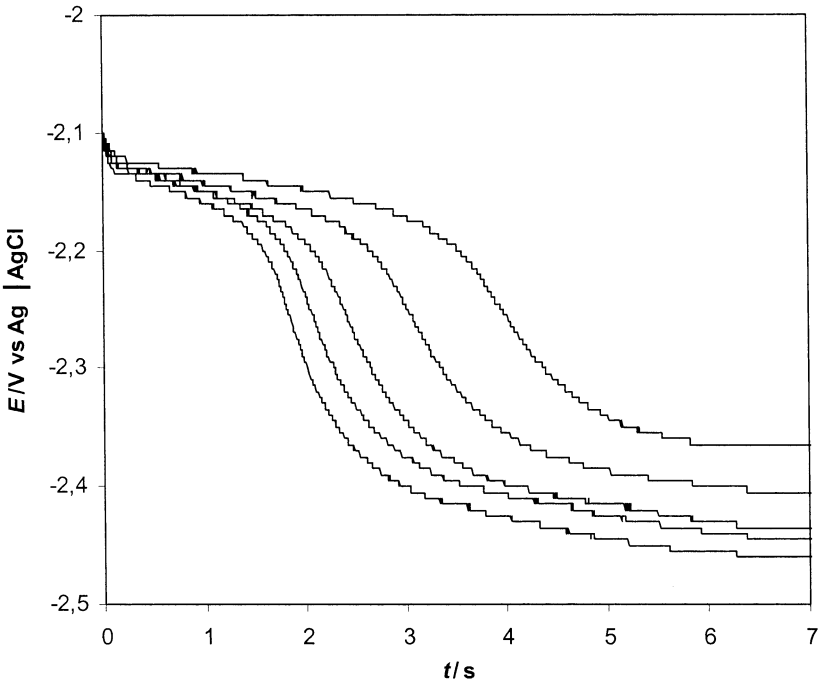

Fig. 7. Example of typical chronopotentiometric curves obtained in the equimolar $CaCl_2$–NaCl mixture at 550 °C containing a RE(III) solution (in this case 9.8621×10^{-5} mol cm^{-3} YCl_3). Tungsten working electrode ($S = 0.38$ cm^2).

In the case of neodymium, the chemical reaction [37]:

$$2\mathrm{Nd(III)} + \mathrm{Nd(0)} \Leftrightarrow 3\mathrm{Nd(II)} \quad (8)$$

prevents the potentiometric determination of the standard potentials of Nd(III)/Nd(II) and Nd(II)/Nd(0) systems. These values were extracted from voltammetric experiments by assuming:

- Reversible behaviour of the electrochemical systems. Then voltammetric curves obtained at low sweep rates (< 200 mV s^{-1}) were analyzed.
- Both systems are separate enough to consider them as independent electrochemical exchanges. As it was shown previously (Fig. 6a and b), this is not strictly correct in the case of the eutectic LiCl–KCl melt, so in this case we will obtain an approximate value.
- The absence of perturbation phenomena, such as nucleation and crystal growth, that introduces an additional overpotential.

The standard potential of the soluble–soluble Nd(III)/Nd(II) system, E_2^o, was determined by voltammetry:

(1) By means of [38]:

$$E_2^o \cong E_{1/2} = \frac{E_p^c + E_p^a}{2} \quad (9)$$

where $E_{1/2}$ is the half-wave potential and E_p^c and E_p^a are the cathodic and the anodic peak potentials, respectively.

Table 2
Values of the standard potential of the RE(III)/RE(0) couples obtained in both molten media

	E^o/V, molality scale versus Cl_2/Cl^- reference	
	Eutectic mixture LiCl–KCl at 450 °C	Equimolar $CaCl_2$–NaCl melt at 550 °C
La(III)/La(0)	−3.183 ± 0.022 [this work] −3.164 [43] −3.177 [51] −3.159 [52] −3.206 [54]	−3.122 ± 0.027 [this work]
Ce(III)/Ce(0)	−3.153 ± 0.005 [this work] −3.151 [43] −3.158 [53,54] −3.216 [55]	−3.035 ± 0.004 [this work]
Nd(III)/Nd(II)	−3.089 ± 0.001 [this work] −3.098 ± 0.010 [43]	−2.873 ± 0.002 [this work]
Nd(II)/Nd(0)	−3.206 ± 0.003 [this work] −3.120 ± 0.015 [43]	−3.163 ± 0.004 [this work]
Pr(III)/Pr(0)	−3.157 ± 0.007 [this work] −3.146 [43,54] −3.156 [53]	−3.031 ± 0.008 [this work]
Y(III)/Y(0)	−3.169 ± 0.008 [this work] −3.142 [56] −3.156 [43] −3.146 [53] −3.184 [54]	−3.032 ± 0.003 [this work]

(2) By simulation of the voltammetric curves by the M271 COOL Kinetic Analysis Software program (from PAR).

(3) By logarithmic analysis of the convoluted voltammetric curves, by applying the equation [38]:

$$E = E_2^{\circ} + \frac{2.3RT}{F}\log\frac{m^* - m}{m} \tag{10}$$

where m is the convoluted current and m^* its limiting value. We assume that, the diffusion coefficients of Nd(III) and Nd(II) species are identical.

The following equation:

$$E_p^c = E_3^{\circ} + \frac{2.3RT}{2F}\log c_o - 0.849\frac{RT}{2F} \tag{11}$$

was applied to determine the standard potential of the Nd(II)/Nd(0) electrochemical exchange, E_3°, c_o being the concentration of electroactive species in solution, Nd(II), which is assumed to be equal to the initial Nd(III) added [39].

The values given in Table 2 correspond to the average of the values obtained in several experiments by using the two different types of RE–working electrodes mentioned previously. Moreover in the case of neodymium an average of the values obtained by the different methods is considered. In the case of the eutectic LiCl–KCl melt, the values were compared to those found in the literature.

In addition, the standard potentials of the different electrochemical exchanges were determined experimentally at different temperatures (Table 3). Taking into account:

$$\Delta G^{\circ} = 3FE^{\circ}_{1RE(III)/RE(0)} \tag{12}$$

the standard Gibbs energy of formation of $RECl_3$ at different temperatures could also be calculated (Table 3).

The fact that the standard potential values of the different RE(III)/RE(0) systems are shifted more positively when increasing the temperature (Table 3), was demonstrated by cyclic voltammetry. Fig. 8 shows, as an example, voltammetric curves obtained in both molten chlorides at different working temperatures, in the case of the La(III)/La(0) system.

Moreover, the standard enthalpy and entropy of formation of $RECl_3$ (Table 4) could be determined from the plot $\Delta G^{\circ}_{RECl_3}$versus T:

$$\Delta G^{\circ}_{RECl_3} = \Delta H^{\circ}_{RECl_3} - T\Delta S^{\circ}_{RECl_3} \tag{13}$$

Table 3
Values of the standard potential of the RE(III)/RE(0) systems (molar fraction scale) and free energy of formation of $RECl_3$ obtained at different temperatures in both molten chlorides

	Eutectic mixture LiCl–KCl			Equimolar $CaCl_2$–NaCl melt		
	T/K	$E^{\circ}_{RE(III)/RE(0)}$/V versus Cl_2/Cl^-	ΔG°_{RECl3}/kJ mol^{-1}	T/K	$E^{\circ}_{RE(III)/RE(0)}$/V versus Cl_2/Cl^-	ΔG°_{RECl3}/kJ mol^{-1}
La(III)/La(0)	673	−3.159	−914.5	823	−3.060	−885.9
	723	−3.124	−904.4	873	−3.012	−872.0
	773	−3.095	−896.0	923	−2.972	−860.4
Ce(III)/Ce(0)	673	−3.125	−904.7	823	−2.978	−862.1
	723	−3.092	−895.1	873	−2.952	−854.6
	773	−3.054	−884.2	923	−2.904	−840.7
	823	−3.018	−873.8	–	–	–
Nd(III)/Nd(0) [a]	673	−3.151	−912.2	823	−3.006	−870.2
	723	−3.105	−898.8	873	−2.972	−860.4
	773	−3.079	−891.3	923	−2.923	−846.2
	823	−3.055	−884.4	–	–	–
Pr(III)/Pr(0)	673	−3.123	−904.1	823	−2.972	−860.4
	723	−3.097	−896.6	873	−2.945	−852.6
	773	−3.060	−885.9	923	−2.903	−840.4
	823	−3.029	−876.9	–	–	–
Y(III)/Y(0)	673	−3.135	−907.5	823	−2.973	−860.2
	723	−3.108	−900.0	873	−2.931	−848.4
	773	−3.082	−892.1	923	−2.902	−840
	823	−3.054	−884.1	–	–	–

[a] Calculated from the equation:

$$E^{\circ}_{Nd(III)/Nd(0)} = \frac{E^{\circ}_{Nd(III)/Nd(II)} + E^{\circ}_{Nd(II)/Nd(0)}}{3}.$$

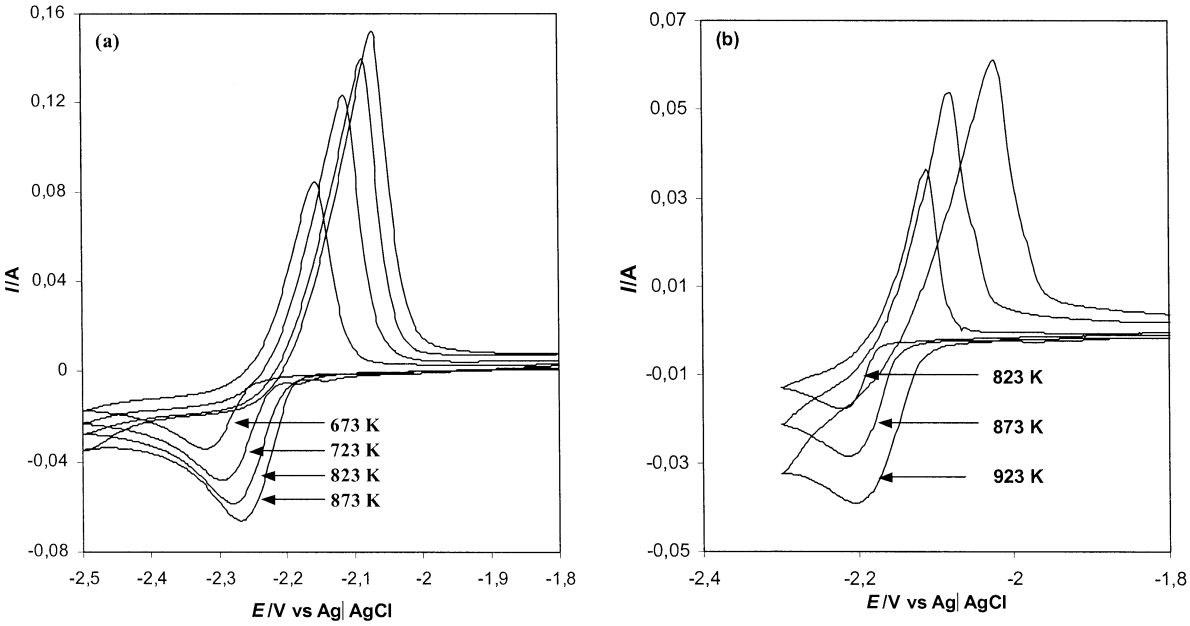

Fig. 8. Cyclic voltammograms of $LaCl_3$ solutions in (a) the eutectic LiCl–KCl and (b) the equimolar $CaCl_2$–NaCl mixture, obtained on a tungsten electrode at different working temperatures.

Table 4
Enthalpy and entropy of formation of $RECl_3$

	Eutectic mixture LiCl–KCl		Equimolar $CaCl_2$–NaCl	
	ΔH/kJ mol^{-1}	ΔS/kJ mol^{-1}	ΔH/kJ mol^{-1}	ΔS/kJ mol^{-1}
$LaCl_3$	−1045.3	−0.1856	−1095.2	−0.2548
$CeCl_3$	−1042.9	−0.2055	−1039.5	−0.2142
$NdCl_3$	−1061.2	−0.2220	−1068.7	−0.2403
$PrCl_3$	−1029.0	−0.1847	−1025.5	−0.1998
YCl_3	−1012.3	−0.1556	−1025.9	−0.2021

3.2.3. Activity coefficients of RE(III)

The activity coefficient of $RECl_3$, γ_{RECl_3}, in the studied melts (Table 5) could be calculated by means of the equation:

$$\log\gamma_{RECl_3} = \frac{3FE_1^{o} - \Delta G^{*}_{fRECl_3SCliq}}{2.3RT} \quad (14)$$

The hypothetical supercooled liquid was chosen as the reference state. $\Delta G^{*}_{fRECl_3SCliq}$ corresponds to the reaction between the pure compounds:

Table 5
Values of the $RECl_3$ activity coefficients obtained in both molten chlorides at different temperatures

Element	T/K	$\Delta G^{*}_{fRECl3Scliq}$ /kJ mol^{-1}	LiCl–KCl				$CaCl_2$–NaCl			
			$E^0_{1(x)}$/V	$E^0_{1(m)}$/V	log γ		$E^0_{1(x)}$/V	$E^0_{1(m)}$/V	log γ	
					Mol fraction scale	Molality scale			Mol fraction scale	Molality scale
Ce	723	−859.919	−3.092	−3.153	−2.542	−3.817				
	823	−840.528	−3.018	−3.095	−2.104	−3.509	−2.978	−3.035	−1.370	−2.416
La	723	−872.976	−3.124	−3.183	−2.268	−3.501				
	823	−836.764	–	–	–	–	−3.060	−3.122	−1.981	−3.119
Nd	723	−850.188	−3.105	−3.167	−3.516	−4.812				
	823	−831.513	−3.055	−3.125	−3.355	−4.640	−3.006	−3.066	−2.456	−3.557
Pr	723	−861.711	−3.097	−3.157	−2.517	−3.771				
	823	−843.325	−3.029	−3.097	−2.129	−3.379	−2.972	−3.031	−1.082	−2.166
Y	723	−820.979	−3.108	−3.169	−5.687	−6.962				
	823	−800.929	−3.054	−3.122	−5.276	−6.525	−2.972	−3.032	−3.789	−4.872

$$RE(s) + 3/2\ Cl_2(g) \Leftrightarrow RECl_3(SCliq) \quad (15)$$

and was derived from Ref. [40].

The activity coefficient gives an idea of the cation complexation by both molten chlorides. According to the results obtained one can say that in the equimolar $CaCl_2$–NaCl melt, the RE(III) ions are less complexed by the chloride ions than in the eutectic LiCl–KCl. This could be explained by the formation of the $CaCl_4^{2-}$ complex [41,42] which leads to less chloride ions free in the calcium melt in comparison to the molten LiCl–KCl mixture. According to this, it can be predicted that the chlorocomplexes formation will occur according to the reactions:

$$RE(III) + 6Cl^- \Leftrightarrow RECl_6^{3-} \quad (16)$$

$$RE(III) + 2CaCl_4^{2-} \Leftrightarrow RECl_6^{3-} + 2Ca(II) + 2Cl^- \quad (17)$$

in the eutectic LiCl–KCl melt (Eq. (16)) and in the equimolar $CaCl_2$–NaCl mixture (Eq. (17)), respectively.

The complexation power also depends on the nature of the cation, its ionic radius and the working temperature. From the values it is also possible to say that the cation with lowest ionic radius (Y^{3+}) is the most solvated by the molten chlorides, which is in agreement with the fact that cations with higher q/r (charge to ionic radius) values, i.e. higher polarizability, are more solvated by the media.

3.2.4. Experimental determination of the solubility products of rare earth oxides in the studied melts

The identification of the RE–O compounds that are stable in the melt as well as the determination of their solubility products, was carried out by potentiometric titration using an yttria stabilised zirconia membrane electrode (YSZME) [16,18,43,44].

The emf between the pO^{2-} indicator electrode and the Ag | AgCl reference electrode was measured when successive additions of known amounts of oxide ions were added to the molten chlorides containing the corresponding $RECl_3$ solutions.

Solid Na_2CO_3 and/or BaO were used as the source of free O^{2-} ions, since they lead to the following equilibria:

$$Na_2CO_3(s) \Leftrightarrow 2Na^+ + O^{2-} + CO_2(g) \quad (18)$$

$$BaO(s) \Leftrightarrow Ba^{2+} + O^{2-} \quad (19)$$

which, under the experimental conditions, have been proved to be completely shifted to the right [13,23,28–30]. Continuous stirring with dried Ar was used to help the dissolution of the solid oxide donor.

The emf values showed a single jump at the point corresponding to the stoichiometric precipitation of the oxide compound, that is an equivalence point, x (defined as the ratio of added oxide ion to initial RE(III) concentration) equal to 1 (Fig. 9). This indicates that a single oxy-compound is formed according to the reaction:

$$RE(III) + O^{2-} + Cl^- \Leftrightarrow REOCl(s) \quad (20)$$

RE being La, Ce, Nd, Pr. The reaction product (REOCl) was also confirmed by XRD analysis of the solid recovered at the end of the experiments.

The solubility products of the different REOCl compounds were calculated by means of the theoretical equation corresponding to the titration curve:

$$E = k + \frac{2.3RT}{2F} pO^{2-} = k + \frac{2.3RT}{2F}\left[-\log\frac{c_o(x-1) + \sqrt{c_o^2(x-1)^2 + 4k_{s(REOCl)}}}{2}\right] \quad (21)$$

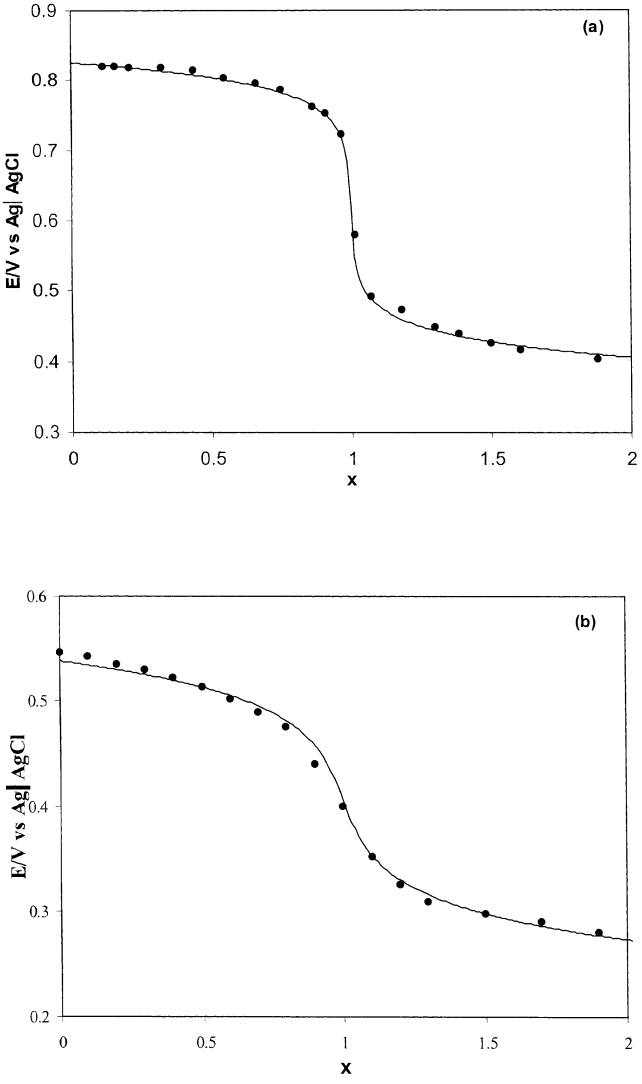

Fig. 9. Experimental values obtained in the potentiometric titration with O^{2-} ions of: (a) La(III) solution (0.1870 mol kg^{-1}) in the eutectic LiCl–KCl at 450 °C; (b) Pr(III) solution (0.07030 mol kg^{-1}) in the equimolar $CaCl_2$–NaCl at 550 °C.

Table 6
Values of the solubility product of REOCl compounds (molality scale) in both molten chlorides

	Eutectic mixture LiCl–KCl at 450 °C	Equimolar $CaCl_2$–NaCl at 550 °C
LaOCl	7.00±0.09	5.19±0.05
CeOCl	7.45±0.05	5.62±0.07
NdOCl	7.67±0.24	5.80±0.31
PrOCl	7.45±0.25	5.46±0.08

where c_o is the initial concentration of RE(III) and k the constant of the YSZME as explained elsewhere [16]. The values so obtained are given in Table 6.

In the case of yttrium in the eutectic LiCl–KCl melt, the emf jump occurs at an equivalence point $x = 1.5$ (Fig. 10), showing that the reaction that takes place is:

$$2Y^{3+} + 3O^{2-} \Leftrightarrow Y_2O_3(s) \quad (22)$$

The theoretical equations corresponding to the titration curve are different from before:

$$[O^{2-}]_{total} = [O^{2-}]_{free} + 3[Y_2O_3]_{precipitated} \quad (23)$$

$$[Y(III)]_{totaladded} = [Y(III)]_{free} + 2[Y_2O_3]_{precipitated} \quad (24)$$

Taking into account the solubility product derived for reaction Eq. (22):

$$K_{s2} = [Y(III)]^2[O^{2-}]^3 \quad (25)$$

it is then possible to develop the theoretical titration curve, which is:

$$[O^{2-}]^5 - 2c_o(x-\tfrac{3}{2})[O^{2-}]^4 + c_o^2(x-\tfrac{3}{2})^2[O^{2-}]^3 - 9/4K_{s2} = 0 \quad (26)$$

c_o being the initial YCl_3 concentration.

The K_{s2} value was determined from the experimental points obtained before the equivalence point (that is $x < 1.5$), where Eq. (26) can be written as follows:

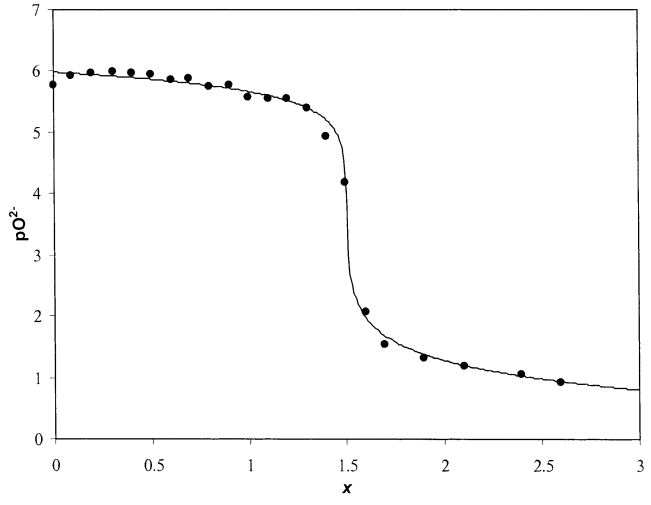

Fig. 10. Potentiometric titration of an Y(III) solution (0.1040 mol kg^{-1}) in the eutectic LiCl–KCl at 450 °C.

$$pO^{2-} = -\tfrac{1}{3}\log\left[\frac{K_{s2}}{c_o^2(1-\tfrac{2}{3}x)^2}\right] \quad (27)$$

The average value obtained in different experiments was 19.90±0.22 (molality scale).

Instability of Ce(IV) and Pr(IV) prevents the experimental determination of the solubility product of CeO_2 and PrO_2 compounds.

Furthermore it is possible to determine theoretically the solubility product of RE_2O_3 (RE ≠ Y) from the standard potentials of the couples:

$$RE_2O_3 + 6e^- \Leftrightarrow 2RE + 3O^{2-} \quad E_4^o \quad (28)$$

$$RE(III) + 3e^- \Leftrightarrow RE \quad E_1^o \quad (29)$$

by means of

$$pK_s(RE_2O_3) = \frac{6F}{2.3RT}(E_1^o - E_4^o) \quad (30)$$

The values obtained showed the instability of RE_2O_3 (RE ≠ Y), as was shown above by potentiometric titration results.

3.2.5. E–pO^{2-} diagrams. Solubilization conditions for RE–O compounds

Solubilization conditions of oxide samples can be theoretically predicted by comparison of the potential–acidity (E–pO^{2-}) diagrams of RE–O compounds stable in the molten solutions and that of some chlorinating mixtures, previously determined [10,11,18,20].

All the data and information (stable oxidation states, standard potential values and solubility products of RE–O compounds) obtained above allow us to build up the E–pO^{2-} diagrams for the RE–O compounds, which summarize the properties of RE–O compounds stable in the molten chlorides studied.

It is also necessary to determine the standard potentials of the different redox systems. Table 7 shows as an example the equations used in the case of Pr. The values of a_{LiCl}, a_{NaCl}, $\log \gamma_{Na_2O}$ and $\log \gamma_{Li_2O}$, were calculated previously [13,20].

Figs. 11a and b show the corresponding E–pO^{2-} diagram obtained in the case of neodymium in both molten chlorides. The figures also show the predominance areas of different chlorinating mixtures.

From the diagrams one can extract the corresponding chlorinating conditions taking into account that:

- A chlorinating mixture whose predominance area corresponds to that of an oxide, will not chlorinate the RE–O compound.
- A chlorinating mixture whose predominance area corresponds to that of a soluble or volatile chloride, will chlorinate the RE–O compound by solubilization or volatilization.

Table 7
Equations corresponding to the standard potentials of the different redox systems necessary for the calculation of $E-pO^{2-}$ diagram of Pr–O compounds

System	Reaction between pure compounds	E_n^o/V
$PrOCl+3e^- \Leftrightarrow Pr+O^{2-}+Cl^-$	–	$E_2^o = E_1^o - \frac{2.3RT}{3F} pK_{CeOCl}$
$Pr_2O_3+6e^- \Leftrightarrow 2Pr+3O^{2-}$	$Pr_2O_3+6ACl \Leftrightarrow 2Pr+3A_2O+3Cl_2$	$E_3^o = -\Delta E_3^* - \frac{2.3RT}{F}\log a_{ACl} + \frac{2.3RT}{2F}\log \gamma_{A_2O}$
$PrO_2+2e^- \Leftrightarrow Pr_2O_3+O^{2-}$	$PrO_2+2ACl \Leftrightarrow Pr_2O_3+A_2O+Cl_2$	$E_4^o = -\Delta E_4^* - \frac{2.3RT}{F}\log a_{ACl} + \frac{2.3RT}{2F}\log \gamma_{A_2O}$
$PrO_2+Cl^-+e^- \Leftrightarrow PrOCl+O^{2-}$	–	$E_4^o + \frac{2.3RT}{2F}\left(\frac{pK_{s1}}{pK_{s2}}\right)$
$PrO_2+e^- \Leftrightarrow Pr(III)+O^{2-}$	–	$E_5^o + \frac{2.3RT}{2F} pK_{s2}$

ΔE_n^* the values thermodynamic potential of the reaction 'n' between the pure compounds extracted from Ref. [15]. ACl and A_2O are the alkali chloride and oxide respectively (LiCl and Li_2O in the case of the LiCl–KCl melt and NaCl and Na_2O in the case of $CaCl_2$–NaCl mixture).

According to this, the chlorinating conditions of Nd–O compounds are given in Table 8.

3.3. Experimental verification of the thermodynamic predictions

Experimental solubilization tests of RE–O compounds (commercial or generated in situ) were performed using different chlorinating agents. The progress of the solubilization reaction was followed by the YSZME when commercial HCl(g) or Cl_2(g) were used, and the final solutions were checked by one of these methods: (i) voltammetry using the standard additions method, (ii) potentiometric titration of the final solution, (iii) taking samples and analyzing by ICP.

3.3.1. Use of HCl(g) in the solubilization of RE–O samples

Table 9 gives the results obtained in the solubilization experiments of RE–O samples of different sizes in both molten chlorides, when using gaseous HCl in an open circuit by means of an alumina tube without a glass frit. Some of the samples used were obtained in situ by precipitation of the corresponding RE(III) solution by O^{2-} ions.

Fig. 12 shows some pictures taken from the experimental cell before and after the solubilization procedure.

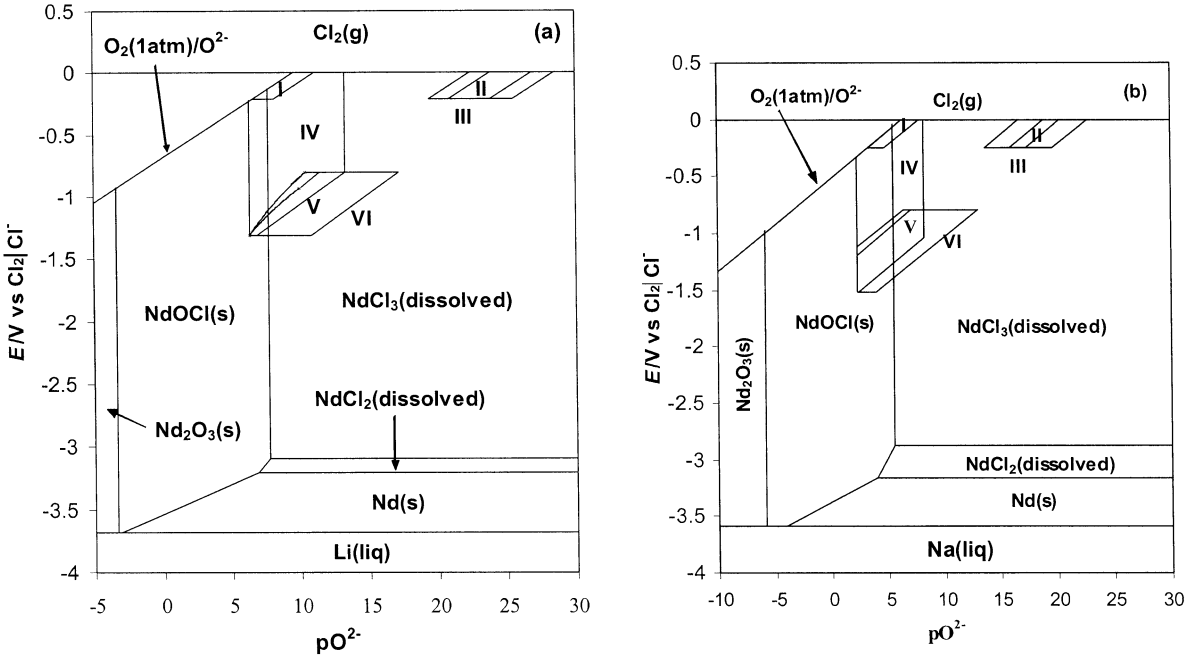

Fig. 11. $E-pO^{2-}$ diagram obtained in the case of NdO compounds in, (a) the eutectic LiCl–KCl at 450 °C; (b) the equimolar $CaCl_2$–NaCl mixture at 550 °C. Concentrations of Nd(III) and Nd(II) assumed equal to 1 mol kg^{-1}. The chlorinating mixtures are; (I) $Cl_2(g)+O_2(g)$, (II) $Cl_2(g)+C(s)$, (III) $Cl_2(g)+CO(g)$, (IV) $HCl(g)+H_2O(g)$, (V) $HCl(g)+H_2(g)+H_2O(g)$, (VI) $HCl(g)+H_2(g)+CO(g)$.

Table 8
Chlorinating conditions of Nd–O compounds extracted from the corresponding E–pO^{2-} diagram (Fig. 11)

Mixture	Chlorinating reactions	Conditions
(I) $Cl_2(g)+O_2(g)$	$2NdOCl(s)+2Cl_2(g)\Leftrightarrow 2NdCl_3(ds)+O_2(g)$ $2Nd_2O_3(s)+6Cl_2(g)\Leftrightarrow 4NdCl_3(ds)+3O_2(g)$	Almost at every pressure of the gases
(II) $Cl_2(g)+C(s)$	$2NdOCl(s)+3Cl_2(g)+C(s)\Leftrightarrow 2NdCl_3(ds)+CO_2(g)$ $2Nd_2O_3(s)+6Cl_2(g)+3C(s)\Leftrightarrow 4NdCl_3(ds)+3CO_2(g)$	At every P of the gases
(III) $Cl_2(g)+CO(g)$	$NdOCl(s)+Cl_2(g)+CO(g)\Leftrightarrow NdCl_3(ds)+CO_2(g)$ $Nd_2O_3(s)+3Cl_2(g)+3CO(g)\Leftrightarrow 2NdCl_3(ds)+3CO_2(g)$	At every P of the gases
(IV) $HCl(g)+H_2O(g)$	$NdOCl(s)+2HCl(g)\Leftrightarrow NdCl_3(ds)+H_2O(g)$ $Nd_2O_3(s)+6HCl(g)\Leftrightarrow 2NdCl_3(ds)+3H_2Og)$	Almost at every P of the gases
(V) $HCl(g)+H_2O(g)+H_2(g)$	$NdOCl(s)+2HCl(g)\Leftrightarrow NdCl_3(ds)+H_2O(g)$ $Nd_2O_3(s)+6HCl(g)\Leftrightarrow 2NdCl_3(ds)+3H_2Og)$	Almost at every P of the gases
(VI) $HCl(g)+CO(g)+H_2(g)$	$NdOCl(s)+2HCl(g)+CO(g)\Leftrightarrow NdCl_3(ds)+CO_2(g)+H_2(g)$ $Nd_2O_3(s)+6HCl(g)+3CO(g)\Leftrightarrow 2NdCl_3(ds)+3CO_2(g)+3H_2(g)$	Almost at every P of the gases

The notation (ds) means (dissolved).

Table 9
Results obtained in the solubilization experiments of RE–O samples when using gaseous HCl

Sample	Sample/g	t_{sol}/min	MELT	Efficiency %
LaOCl	3.4223	50.0	LiCl–KCl at 450 °C	100
	1.2149	–	$CaCl_2$–NaCl at 550 °C	99
La_2O_3	0.7320	9.0	LiCl–KCl at 450 °C	100
	2.9376	18.0	LiCl–KCl at 450 °C	98
	0.7331	32.0	LiCl–KCl at 450 °C	98.8
	1.1417	–	$CaCl_2$–NaCl at 550 °C	98
	0.9684	22.0	$CaCl_2$–NaCl at 550 °C	98
	0.4957	44.0	$CaCl_2$–NaCl at 550 °C	100
CeOCl	0.6984	22.0	LiCl–KCl at 450 °C	100
	0.6634	30.0	$CaCl_2$–NaCl at 550 °C	100
CeO_2	0.7264	25.0	LiCl–KCl at 450 °C	100
	0.7458	30.0	$CaCl_2$–NaCl at 550 °C	100
PrOCl	1.3798	18.0	LiCl–KCl at 450 °C	100
	0.6694		$CaCl_2$–NaCl at 550 °C	100
Pr_6O_{11}	0.8215	35.0	LiCl–KCl at 450 °C	98
	0.6323	26.0	LiCl–KCl at 450 °C	100
	0.4005	20.0	LiCl–KCl at 450 °C	100
	0.3087	7.0	LiCl–KCl at 450 °C	100
	0.7458	30.0	$CaCl_2$–NaCl at 550 °C	100
NdOCl	1.1198	25.0	LiCl–KCl at 450 °C	100
	0.4324	17.0	$CaCl_2$–NaCl at 550 °C	100
Nd_2O_3	0.9024	35.0	LiCl–KCl at 450 °C	100
	0.7551	32.0	LiCl–KCl at 450 °C	95
	0.7556	40.0	$CaCl_2$–NaCl at 550 °C	100
	0.8932	36.0	$CaCl_2$–NaCl at 550 °C	100
Y_2O_3	0.3790	17.0	LiCl–KCl at 450 °C	99.7
	0.3712	18.0	LiCl–KCl at 450 °C	100
	0.5375	25.0	LiCl–KCl at 450 °C	100
	0.4516	10.0	$CaCl_2$–NaCl at 550 °C	100

t_{sol} is the solubilization time.

3.3.2. Use of $Cl_2(g)$ in the solubilization of RE–O samples

Experimental results when using pure $Cl_2(g)$ as the chlorinating agent shows that the time required for the solubilization of RE–O samples is much higher than that for gaseous HCl(g). In this case, the experiments were carried out in the eutectic LiCl–KCl melt with Nd_2O_3 and Y_2O_3 samples (Table 10). The Cl_2 was bubbled through an alumina tube or a Pyrex tube with a glass frit at the end (porosity 100–160 μm).

The results could be explained by the different kinetics of the solubilization reaction for HCl(g) and $Cl_2(g)$, since according to the thermodynamic predictions extracted from the E–pO^{2-} diagrams, commercial gaseous $Cl_2(g)$ imposes pO^{2-} values high enough to allow solubilization of RE–O samples.

The solubilization reaction of metal oxides has been proposed to occur in two steps [45]:

1) Dissolution of the chlorinating agent in the molten chloride.
2) Diffusion of the dissolved chlorinating agent to the metal oxide.

The kinetics of the first step depend on the chlorinating gas. The second step is influenced by the chlorinating gas and also the nature of the molten chloride. Both steps are dependent on the working temperature.

Novozhilov et al. [46] showed that dissolution of $Cl_2(g)$ in NaCl–KCl is a physical process similar to that corresponding to inert gasses. However, the dissolution of gaseous HCl occurs through formation of complexes HCl_x^{1-x} (x being between 3 and 4). In this way, these authors indicated that dissolution of HCl(g) is faster than that of $Cl_2(g)$.

In addition Minh and Welch [47] and Van Norman and Tivers [48,49] proved that solubility of HCl(g) is 7

Table 10
Results obtained in the solubilization experiments of RE–O samples when using gaseous Cl_2

Sample	Sample/g	t/min	Efficiency %
Y_2O_3	0.1003 (a)	250	100 (CV)
	0.2010 (b)	120	95 (CV)
Nd_2O_3	0.1441 (a)	300	< detection limit by CV
	0.6670 (b)	15	8 (ICP)
	0.6670 (b)	30	8 (ICP)
	0.6670 (b)	60	14 (T) 12 (ICP)
	0.6009 (b)	36	20 ICP
	0.1202 (b)	105	48 (CV)

CV, standard addition method; T, Titration of the final solution; ICP, ICP Spectrometry; t, is the total time of the chlorinating treatment; Cl_2, bubbled through; (a) an alumina tube, (b) a Pyrex tube with glass frit.

times higher than that of Cl_2(g) in the LiCl–KCl melt at 450 °C.

Moreover diffusion coefficients of HCl(g) and Cl_2(g) in molten chlorides found in Refs. [13,50] lead to the same results: the solubilization reaction of metal oxides with HCl(g) is more favourable than with Cl_2(g).

3.3.3. Use of the $Cl_2(g)+C(s)$ chlorinating mixture in the solubilization of RE–O

The chlorinating power of the Cl_2(g)+C(s) chlorinating mixture (mixture II) was tested. The process is well known in the industry, but working at higher temperatures ($T > 1000$ °C), and it is known as 'carbochlorination'.

In this case, the chlorinating power of the gaseous Cl_2 is increased by combining a reductant agent such as the solid carbon, which reacs very easily with O^{2-} ions to form CO_2(g).

In this case only the eutectic LiCl–KCl melt at 2 temperatures, 450 and 700 °C, was tested. Glassy carbon or alumina crucibles were used as the electrolyte container, and the Cl_2 was bubbled through an alumina or graphite tube. The RE–O samples were very well mixed with a stoichiometric excess of carbon fine powder (Aldrich 1–2 μm). An active carbon filter was connected in the gas-out line.

The results obtained in the chlorination of commercial Nd_2O_3, Y_2O_3 and La_2O_3 samples are given in Table 11, and show that the presence of carbon increases the kinetics of the chlorinating reaction of gaseous chlorine. Even better kinetics could be obtained when the temperature was increased.

4. Conclusions

The equilibrium constant of the acid–base HCl/H_2O system, $K_{H_2O/HCl}$, was determined in the eutectic LiCl–KCl mixture at 450 °C and in the equimolar $CaCl_2$–NaCl melt at 550 °C, showing the different oxoacidic properties of both molten chlorides. This was done by measuring the emf between the reference and an oxide ion selective electrode made of an yttria-stabilized membrane with different partial pressures of gaseous HCl and H_2O, which was achieved by bubbling Ar through thermostated HCl aqueous solutions.

The response of the YSZME was Nernstian over a wide range, and the potential values could be related to pO^{2-} by knowing the equation of the electrode, which was possible after its calibration by successive additions of solid Na_2CO_3 or BaO.

Stable oxidation states of La, Ce, Pr and Y were found to be (III) and (0) in both molten chlorides. In the case of neodymium, oxidation state (II) was also found to exist being more stable in the calcium melt. In the case of cerium and praseodymium, voltammetric curves did not show any anodic signals apart from that at the upper limit of the melts (chlorine evolution), indicating the oxidizing behaviour of Ce(IV) and Pr(IV) species,

Table 11
Results obtained in the solubilization experiments of RE–O samples when using the Cl_2 (g)+C (s) gaseous mixture

Sample	Sample/g	Solid C/g	t/min	T/°C	Efficiency %
Nd_2O_3	0.9063	0.4162	60	450	30 (CV)
	0.9014	0.4036	90	450	43(ICP)
	0.9002	0.4377	120	450	50(T)
	0.9063	0.4162	240	450	94 (CV) 93(ICP)
	0.9270	0.4100	30	700	26 (T) 27 (ICP)
	0.9000	0.1476	50	700	40 (T) 45 (ICP)
	0.9003	0.4070	80	700	72 (T) 72(ICP)
	0.9063	0.5021	120	700	98 (CV)
La_2O_3	0.6008	0.4610	30	700	49 (T)
	0.6060	0.4841	50	700	66 (T)
	0.6001	0.5460	90	700	98 (CV)
Y_2O_3	0.3555	0.5200	60	700	97 (CV)

CV, standard addition method; T, Titration of the final solution; ICP, ICP Spectrometry; t, is the total time of the chlorinating treatment.

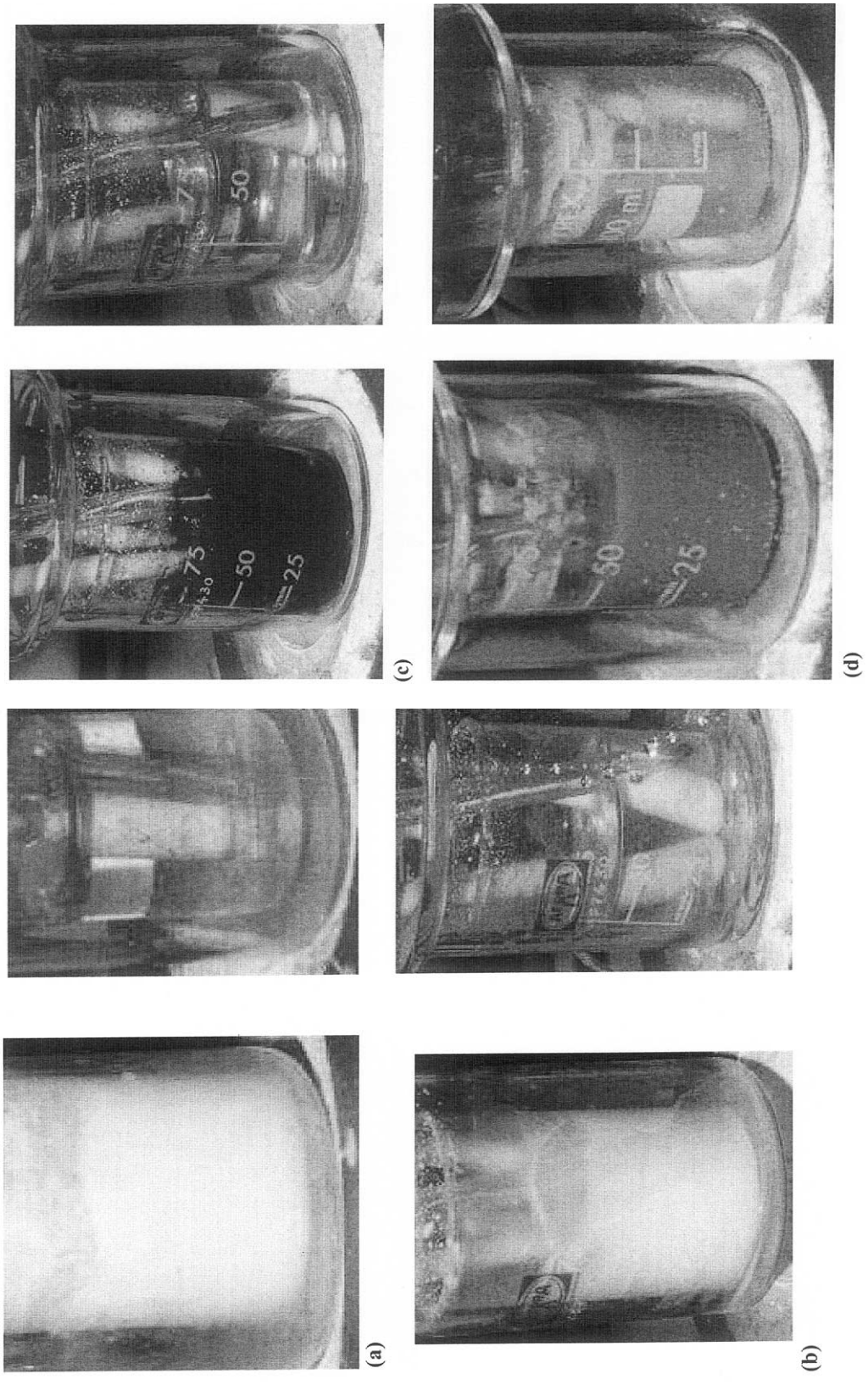
75
50
25
(a)
(b)
(c)
(d)

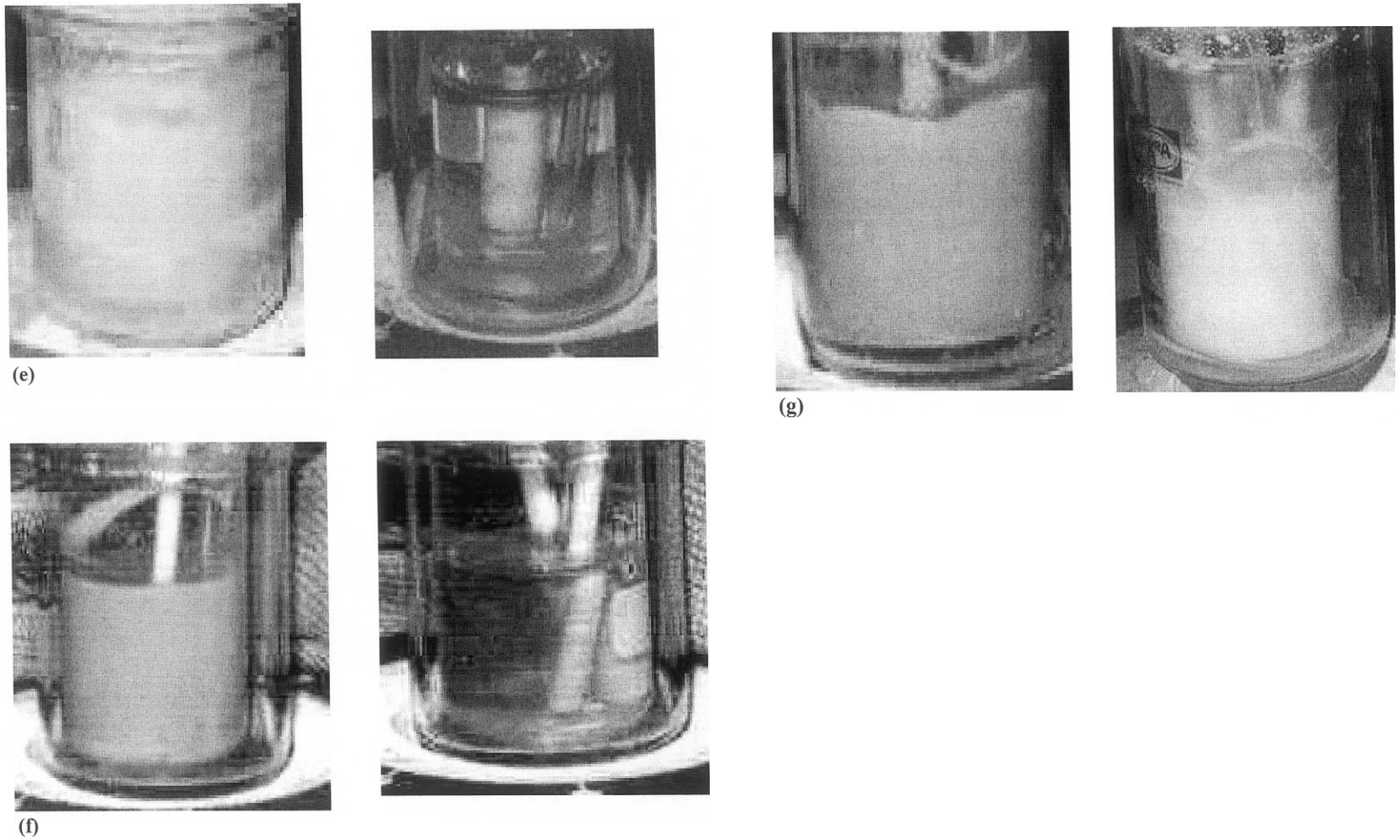

Fig. 12. Pictures taken from the experimental cell before and after the solubilization procedure with gaseous HCl. a La2O3 sample in the eutectic LiClKCl at 450C; b PrOCl sample in the eutectic LiClKCl at 450C; c Pr6O11 sample in the eutectic LiClKCl at 450C; d Pr6O11 sample in the equimolar CaCl2NaCl at 550C; e Y2O3 sample in the eutectic LiClKCl at 450C; f CeO2 sample in the eutectic LiClKCl at 450C; g CeO2 sample in the equimolar CaCl2NaCl at 550C.

which react with the chlorides of the melt according to:

$$2Cl^- + 2Ce(IV) \text{ or } Pr(IV) \Leftrightarrow Cl_2(g) + 2Ce(III) \text{ or } Pr(III)$$

The standard potentials of the different RE(III)/Re(0) redox couples were determined by potentiometric measurement of the emf between the Ag | AgCl reference and a RE electrode in solutions of the molten chlorides containing different RE(III) concentrations. Extrapolation of measured values of E to $x_{RECl_3} = 1$ or $c_{RECl_3} = 1\ \text{mol kg}^{-1}$ permits the calculation of E_x^o or E_m^0 respectively.

In the case of neodymium, the reaction:

$$2Nd(III) + Nd(0) \Leftrightarrow 3Nd(II)$$

prevents potentiometric determination of the standard potential of the Nd(III)/Nd(0) couple. E^o of the Nd(III)/Nd(II) and Nd(II)/Nd(0) systems were determined by different electrochemical techniques (i.e. cyclic voltammetry and convolution analysis) by means of the appropriate equations and assuming a reversible behaviour of the systems.

Variation of the standard potentials with the temperature was also studied, yielding a shift towards more positive values when increasing the working temperature.

Knowing the E^o of the different RE(III)/RE(0) systems, it is possible to determine the Gibbs energy of formation of $RECl_3$, and by comparison to that from the pure compounds one can calculate the activity coefficients of $RECl_3$ compounds. The results showed that the rare earth cations are more solvated by the molten chlorides in the lithium melt than in the calcium mixture, which leads to the conclusion that in the first melt, the solvation reaction could be expressed as:

$$RE(III) + 6Cl^- \Leftrightarrow RECl_6^{3-}$$

whereas in the calcium melt, where the existence of calcium chlorocomplexes is well known, the solvation of RE(III) cations occurs according to:

$$RE(III) + 2CaCl_4^{2-} \Leftrightarrow RECl_6^{3-} + 2Ca(II) + 2Cl^-$$

On the other hand, it is shown that the most polarizable cation Y(III) possesses the lowest activity coefficient, that is, it is the rare earth cation most solvated by the molten chlorides.

Moreover, identification of RE–O compounds stable in the molten chlorides was made by potentiometric titration of RE(III) solutions by O^{2-} ions. The results showed the formation of solid oxychlorides of the type REOCl, RE being La, Ce, Nd and Pr in both molten chlorides studied, and solid Y_2O_3 in the eutectic LiCl–KCl melt. Calculation of the different solubility products was possible.

After building up the E–pO^{2-} diagrams of the RE–O compounds, it is possible to predict the best chlorinating conditions of the oxy-compounds when using different chlorinating mixtures based on gaseous HCl and Cl_2.

Experimental solubilization tests of different rare earth oxy-compounds were performed by using HCl(g), Cl_2(g) and the chlorinating mixture $Cl_2(g) + C(s)$, showing the different kinetics in the solubilization reactions. This was explained by the different solubilization mechanism of the gaseous HCl and Cl_2 as well as by the different diffusion properties of both gases in the molten chlorides. All this led to much lower kinetics in the case of solubilization reactions that use gaseous chlorine. We have observed, in the case of the $Cl_2 + C$ mixture, that an increase of the working temperature leads to higher kinetics, due to the increase in the solubilization of Cl_2(g).

Acknowledgements

The authors thank Francisco de la Rosa (Universidad de Valladolid) and Luis Gutierrez (CIEMAT) for technical assistance, and ENRESA (Spain) for financial support (CIEMAT-ENRESA and CIEMAT-UNIVERSIDAD DE VALLADOLID agreements). A.M.M. wishes to thank the 'Secretaría de Estado de Educacion, Universidades, Investigacion y Desarrollo' (Spain) for a post-doctoral grant. Some aspects of the work were part of the UE PYROREP FIKW-CT-2000-00049 project.

References

[1] D.M. Ferry, G.S. Picard, B.L. Trémilllon, Trans. Instn. Min. Metall. 97 (1988) C21–C30 (Section C: Mineral Process Extr. Metall.).
[2] T. Koyama, M. Iizuka, H. Tanaka, M. Tokiwai, Y. Shoji, R. Fujita, T. Kobayashi, J. Nucl. Sci. Technol. 34 (1997) 384.
[3] T.H. Pigford, Actinide burning and waste disposal, an invited review for the MIT International Conference on the Next Generation of Nuclear Power Technology, Department of Nuclear Engineering, University of California ar Berkeley, CA, UCB-NE-4176, Rev. 1 (October 1990).
[4] M. Tokiwai, T. Kobayashi, T. Koyama, M. Tsunashima, S. Horie, T. Kawaii, I. Kakehi, H. Matsuura, K. Yanagida, M. Shuto, Proceedings of International Conference on Fast Reactors and Related Fuel Cycles (FR'91), October 1991, Kyoto, Japan, Vol. II, (1991) 12.7–1.
[5] M. Iizuka, K. Uozumi, T. Inoue, T. Iwai, O. Shirai, Y. Arai, NEA/OECDE 2000.
[6] T. Inoue, Y. Sakamura., in: M. Gaune-Escard (Ed.), Molten salts: from fundamentals to applications. NATO science series II, vol. 52, Kluwer Academic Publishers, Dordrecht, 2002, pp. 249–261.
[7] Actinide and Fission Product Partitioning and Transmutation. Status and Assessment report. NEA/OCDE, 1999.
[8] J.J. Laidler, Trans. Am. Nucl. Soc. 68 (1993) 16.
[9] Y. Sakamura, T. Inoue, O. Shirai, T. Iwai, Y. Arai, Y. Suzuki, Proceedings of Global 99, Jackson Hole, Wyoming, USA, 1999.
[10] G.S. Picard, Molten Salt Forum, 1–2, 1993/94 25.

[11] G.S. Picard, F.M. Seon, B.L. Tremillon, Proceedings of the Fourth International Symposium on Molten Salts. The Electrochemical Society, Washington, DC, (1984), 694–706.
[12] G.S. Picard, S. Sánchez, D. Lambertín, J. Lacquement, Proceeding of Global 2001. International Conference of the Fuel Cycle: from Research Solutions, Paris, France 2001.
[13] F. Seon, Doctoral Thesis, Paris, 1981.
[14] F. Seon, G. Picard, B. Tremillon, Electrochim. Acta 28 (1983) 209.
[15] M.D. Lambertin, Doctoral Thesis, Paris, 2001.
[16] Y. Castrillejo, M.R. Bermejo, R. Pardo, A.M. Martínez, J. Electroanal. Chem. 522 (2002) 124.
[17] A.M. Martínez, Doctoral Thesis, Valladolid, 1999.
[18] A.M. Martínez, Y. Castrillejo, E. Barrado, G.M. Haarberg, G.S. Picard, J. Electroanal. Chem. 449 (1998) 67.
[19] Y. Castrillejo, A.M. Martínez, M.R. Bermejo, M.S. Vega, G.M. Haarberg, G.S. Picard., in: M. Gaune-Escard (Ed.), Advances in molten salts. From structural aspects to waste processing, Begell Housse, New York, 1999, pp. 78–92.
[20] Y. Castrillejo, M.R. Bermejo, In: Report CIEMAT-University of Valladolid Agreement, 2000.
[21] M.R. Bermejo, Y. Castrillejo, A. Martínez, E. Barrado, Proceeding of Global 2001. International Conference of the Fuel Cycle: from Research Solutions, Paris, France 2001.
[22] H.A. Laitinen, W.B. Ferguson, R.R. Osteryoung, J. Electrochem. Soc. 104 (1957) 516.
[23] Y. Castrillejo, A.M. Martínez, G.M. Haarberg, B. Børresen, K.S. Osen, R. Tunold, Electrochim. Acta 42 (1997) 1489.
[24] G.S. Picard, Doctoral Thesis, Paris, 1973.
[25] B. Tremillon, G.S. Picard, Anal. Chim. Acta 82 (1976) 273.
[26] J. Schenin-King, Doctoral Tesis, Paris, 1994.
[27] R. Combes, B. Tremillon, F. de Andrade, M. Lopes, H. Ferreira, Anal. Lett. 15 (1982) 1585.
[28] International Critical Tables, Vol. III, Vapour Pressure Lowering, p. 292.
[29] G.S. Picard, F. Seon, B. Tremillon, J. Electroanal. Chem. 102 (1979) 65.
[30] B. Trémillon, G. Picard, Proceedings of the First International Symposium on Molten Salt Chemistry and Technology, 1983.
[31] B. Trémillon, Reactions in Solution. An Applied Analytical Approach, Wiley, Chichester, 1997.
[32] R. Lisy, R. Combes, J. Electroanal. Chem. 83 (1977) 287.
[33] L.F. Druding, J.D. Corbett, J. Am. Chem. Soc. 83 (1961) 2462.
[34] L. Feng, C. Guo, D. Tang, J. Alloys Compounds 234 (1996) 183.
[35] F.H. Keneshea, Jr., D. Cubicciotti, J. Chem. Eng. Data 6 (1961) 507.
[36] A.S. Dworkin, H.R. Brostein, M.A. Bredig, Discuss. Faraday Soc. 32 (1962) 188.
[37] I. Wu, H. Zhu, Y. Sato, T. Yamamura, K. Sugimoto, in: C.L. Hussey, D.S. Newman, G. Mamantov, Y. Ito, (ed.), Molten Salts. Ninth International Symposium, Pennington, 1994, 504.
[38] A.J. Bard, L.R. Faulkner, Electrochemical Methods. Fundamentals and Applications, Wiley, New York, 1980.
[39] P. Delahay (Ed.), New Instrumental Methods in Electrochemistry. Theory, Instrumentation, and Applications to Analytical and Physical Chemistry, Interscience, New York, 1954.
[40] J. Barin, O. Knacke (Eds.), Thermochemical Properties of Inorganic Substances, Springer, Berlin, 1973.
[41] K. Igarashi, T. Nijima, J. Mochinaga, Proceedings of the First International Symposium on Molten Salt Chemistry and Technology, 1983, K-203.
[42] V.G. Roewer, H.H. Emons, Z. Anorg. Allg. Chem. 370 (1969) 128.
[43] Y. Mottot, Doctoral Thesis, Paris, 1986.
[44] R. Combes, M.N. Levelut, B. Trémillon, J. Electroanal. Chem. 91 (1978) 125.
[45] J. Schenin-King, G.S. Picard, Molten Salt Forum 1–2 (1993/94) 13.
[46] A.L. Novozhilov, V.N. Devyatkin, E.I. Pchlina, Russ. J. Phys. Chem. 48 (1974) 31.
[47] N.Q. Minh, B.J. Welch, Aust. J. Chem. 28 (1975) 965.
[48] J.D. Van Norman, R.J. Tivers, J. Electrochem. Soc. 118 (1971) 258.
[49] J.D. Van Norman, R.J. Tivers, in: G. Mamantov (Ed.), Molten Salts. Characterization and Analysis, Marcel Dekker, New York, 1969, p. 509.
[50] J. Schenin-King, Doctoral Thesis, Paris, 1994.
[51] F. Lantelme, Y. Berghoute, J. Electrochem. Soc. 146 (1999) 4137.
[52] J. Lesourd, J.A. Plambeck, Can. J. Chem. 47 (1969) 3387.
[53] J.J. Roy, L.G. Grantham, L.R. McCoy, C.L. Krueger, T. Storvick, T. Inoue, H. Miyashiro, N. Takahashi, Mater. Sci. Forum 547 (1991) 73.
[54] S.P. Fusselman, J.J. Roy, D.L. Grimmett, L.G. Grantham, C.L. Krueger, C.R. Nabelek, T.S. Stovick, T. Inoue, T. Hijikata, K. Kinoshita, Y. Sakamura, K. Uozumi, T. Kawai, T. Takahashi, J. Electrohem. Soc. 146 (1999) 2573.
[55] D. Inman, G.J. Hills, L. Young, J. O'M. Brockis, Ann. N.Y. Acad. Sci. 79 (1960) 803.
[56] Y. Hoshino, J.A. Plambeck, Can. J. Chem. 48 (1970) 685.